ISSN 2616-5805 Vol. 5, Issue 3: 23-30, DOI: 10.25236/AJMS.2024.050304

Collision avoidance path planning for unmanned autonomous ships in complex waters

Dawei Chen[a,*], Renqiang Wang[b], Jianming Sun[c], Changhua Liu[d]

College of Navigation, Jiangsu Maritime Institute, Nanjing, China
[a]cdw6015@163.com, [b]wangrenqiang2009@126.com, [c]sjmwj421@163.com, [d]vnd@126.com
[*]Corresponding author
https://orcid.org/0000-0002-2970-2933

Abstract: *A dynamic path planning method for unmanned autonomous ship collision avoidance with velocity potential field is proposed, which solves the problem that the artificial potential field method constructed with distance as an element cannot make the moving body actively redirect to avoid collision. In the artificial potential field, the relative speed between the unmanned ship and the obstacle, and the relative speed between the unmanned ship and the target point are integrated into the potential field, and the distance-speed potential field model is constructed. Adding the velocity potential field to the repulsion potential field can enable the unmanned autonomous ship to actively alter its course to the left or right to avoid collision; adding the velocity potential field to the attractive potential field can enable the unmanned autonomous ship to adjust the speed. The method is applied to the dynamic path planning experiment of unmanned autonomous ship collision avoidance in complex and changeable waters where dynamic and static obstacles coexist. The results show that unmanned autonomous ships can quickly avoid obstacles by actively altering her course, and the algorithm conforms to the actual collision avoidance engineering.*

Keywords: *Collision avoidance, path planning, velocity potential field, unmanned autonomous ships, complex waters*

1. Introduction

The path planning of collision avoidance for ships in complex and changeable waters, such as narrow waterways, is too complicated. Not only must the problem of fixed dangerous objects avoid obstacles in the navigating waters be considered, but also the dynamic collision avoidance problems of other navigating ships [1]. In the design of the path planning system of ship's collision avoidance , it is necessary to fully consider the maneuverability of the unmanned ship itself, the environment of the navigating water area and the interference of the surrounding navigating ships.

At present, at home and abroad, the methods for studying the path planning of collision avoidance of ships in sailing waters. The SI algorithm is to determine the environment including dynamic and static obstacle information through calculation, and calculate the collision-free path according to the mathematical model of ship motion [2]. The DA method [3] and the ML method [4] essentially share the same source, both of which are secondary expert decisions based on previous data [5], combined with ship handling characteristics to solve current or future navigation collision warnings, and then take the action for collision avoidance. The RRT algorithm [6] uses the point random expansion algorithm to achieve the second optimal route, but the optimal route has convex points, which does not conform to the continuous smooth characteristic, and cannot be directly applied to the route planning of the ship moving body. The DW algorithm [7] calculates the speed range and angular velocity through the current speed and heading angle state, and ship motion model, and calculates the reachable position at each speed and angular velocity in this range. Then through the collision evaluation of each position, the optimal position was selected. Essentially the same as the aforementioned DA method and ML method. In the literature [8], the collision avoidance Rules are integrated into the DW model to realize the autonomous collision avoidance of unmanned surface vehicle (USV) with the constraints of the complexity of maritime traffic and other factors. The VO method [9] defines a cone-shaped space on the obstacle and keeps the moving body out of the space to avoid collisions with nearby obstacles. However, in a complex environment such as narrow waterways, it is difficult to achieve the effects of collision avoidance. When there are multiple obstacles in the water, the optimization of speed and

ISSN 2616-5805 Vol. 5, Issue 3: 23-30, DOI: 10.25236/AJMS.2024.050304

heading will produce vibration [10]. Lee [11] incorporated the International Navigation Rules into the VO method, and developed an automatic route generation algorithm of collision avoidance for merchant ships. And the algorithm overcomes the deadlock problem of manual methods.

Compared with these methods, the biggest advantage of the APF method is that the obstacle potential field can be constructed arbitrarily based on human experience, and the potential field force can be integrated into the dynamic model of the moving body, which conforms to the reality of continuous real-time collision avoidance of the moving body [12], but the problem of the speed potential field of the moving body is ignored. As well known, at a certain distance, when the speed between the moving body and the obstacle is greater, the collision is more likely to occur; and, when the angle between the moving body and the obstacle is smaller, the damage caused by the collision is greater. In view of this, on the basis of the aforementioned improved method, this article increases the velocity potential field between the moving body and the obstacle and the target point. An improved artificial potential field, and the method is applied to the planning of the autonomous navigation collision avoidance path of an unmanned ship in a narrow channel, in order to obtain an effective method that conforms to the actual project.

2. Improved APF integrated with velocity vector

2.1. APF model

APF is a virtual force method for robot motion planning proposed by Khatib [13]. The basic idea is to realize the impact of targets and obstacles on the robot's motion into an artificial potential field, with low potential energy at the target and high potential energy at the obstacle. This potential difference produces the harm of the artificial potential field standard to the robot and the repulsive force of obstacles to the robot. The resultant force controls the robot to move to the target point along the direction of the potential field.

The combined potential field is the sum of the attractive potential field and the repulsive potential field:

$$U(x)=U_{att}(x)+U_{rep}(x) \tag{1}$$

Where, $U_{att}(x)$ is the attractive potential field generated by the target; $U_{rep}(x)$ is the sum of the repulsive potential field generated by each obstacle, namely $U_{rep}(x)=\sum_{j=1}^{n}U_{rep,j}(x)$.

The mathematical model of the attractive and repulsive force potential field of the target point and obstacle to the robot is,

$$U_{att}(x)=\frac{1}{2}\xi d^2(x,G) \tag{2}$$

$$U_{rep,j}(x)=\begin{cases}\frac{1}{2}\eta_j\left(\frac{1}{d_j(x)}-\frac{1}{Q_j^*}\right)^2 & d_j(x)\le Q_j^* \\ 0 & d(x,G)>Q_j^*\end{cases} \tag{3}$$

Where, ξ represents the relative influence of the attractive potential; η_j represents the relative influence of the repulsive force of the j-th obstacle, x represents the current position of the robot, G represents the position of the target point, $d(x,G)$ represents the distance between the robot and the target, $d_j(x)$ represents the distance of the robot from the j-th obstacle, Q_j^* represents the range of the repulsive force of the j-th obstacle.

ISSN 2616-5805 Vol. 5, Issue 3: 23-30, DOI: 10.25236/AJMS.2024.050304

2.2. Construction of APF integrating velocity vector

At a certain distance, when the speed between the moving body and the obstacle is greater, the collision is more likely to occur; and, when the angle between the moving body and the obstacle is smaller, the degree of damage caused by the collision is also greater. For this reason, on the basis of the aforementioned improved method, the velocity potential field between the moving body and the obstacle and the target point is increased and integrated into the distance potential field, as shown in Figure 1.

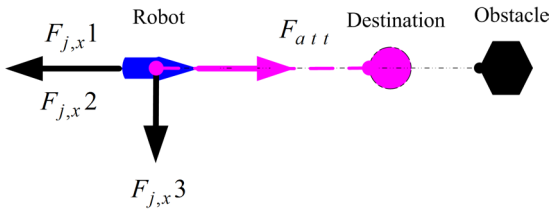

Figure 1: Schematic diagram of merging the velocity potential field

Then, the mathematical expression of the attractive potential field of the target point on the moving body is,

$$U_{att}(x,V)=\begin{cases}\frac{1}{2}\xi d^2(x,G)+\frac{1}{2}\xi_V\left\|V-V_{goa}\right\|^2 & d(x,G)\le d_G^* \\ d_G^*\xi d(x,G)-\frac{1}{2}d_G^*\xi+\frac{1}{2}\xi_V\left\|V-V_{goa}\right\|^2 & d(x,G)>d_G^*\end{cases} \tag{4}$$

Where, the term $\frac{1}{2}\xi_V\left\|V-V_{goa}\right\|^2$ is the attractive potential field considering the speed, ξ_V is the attractive coefficient of the relative speed, V is the current speed of the moving body, and V_{goa} is the ending speed when the moving body reaches the target point. The meanings of other parameters are as mentioned above.

By finding the negative gradient of the attractive potential field function, the attractive force of the target point on the ship can be obtained,

$$F_{att}(x,V)=-\nabla U_{att}(x,V)=\begin{cases}\xi d(x,G)e_{d,att}+\xi_V V_{R,goa}e_{V_{R,goa}} & d(x,G)\le d_G^* \\ d_G^*\xi e_{d,att}+\xi_V V_{R,goa}e_{V_{R,goa}} & d(x,G)>d_G^*\end{cases} \tag{5}$$

Where, $e_{d,att}$ is the unit vector of the current position of our ship pointing to the target point, $V_{R,goa}$ is the relative speed of our ship's current and reaching the target point speed, and $e_{V_{R,goa}}$ is the unit vector of our ship's current speed pointing to the target point.

Similarly, the mathematical expression of the repulsive force potential field of the obstacle to the moving body is,

$$U_{rep,j}(x,V)=\begin{cases}\frac{1}{2}\eta_j\left(\frac{1}{d_j(x)}-\frac{1}{Q_j^*}\right)^2 d(x,G)^2+\frac{1}{2}\eta_V {V_{R,obs}}^2 & d_j(x)\le Q_j^* \\ 0 & d_j(x)>Q_j^*\end{cases} \tag{6}$$

Where, the term $\frac{1}{2}\eta_V {V_{R,obs}}^2$ is the repulsive force field considering the speed, η_V is the relative velocity repulsion coefficient; $V_{R,obs}=(V-V_{obs})^{\mathrm{T}}e_{R,obs}$, V is the current speed of the moving body, and V_{obs} is the moving speed of the obstacle.

ISSN 2616-5805 Vol. 5, Issue 3: 23-30, DOI: 10.25236/AJMS.2024.050304

According to the concept of gradient, $\nabla_R V_{R,obs} = e_{R,obs}$, $\nabla_x V_{R,obs} = \frac{V_{R,obs} \cdot e_{R,obs} - V_{R,obs}}{d_j(x)}$. Let $V_{R,obs\perp} e_{R,obs\perp}$ be the vertical component of $V_{R,obs} \cdot e_{R,obs}$, we can get $V_{R,obs\perp} e_{R,obs\perp} = V - V_{obs} - V_{R,obs} \cdot e_{R,obs}$. Further, we can get, $\nabla_x V_{R,obs} = -\frac{V_{R,obs.\perp}}{d_j(x)}$.

By seeking the negative gradient of the potential field function of the repulsion force, the repulsion force of the obstacle against the ship can be obtained,

$$F_{rep,j}(x,V) = -\nabla U_{rep,j}(x,V) = \begin{cases} F_{j,x} + F_{j,V} & d_j(x) \le Q_j^* \text{ and } V > 0 \\ 0 & d_j(x) > Q_j^* \text{ and } V > 0 \end{cases} \tag{7}$$

Where, $F_{j,x}$ is the repulsive force generated by the potential field of the j-th obstacle position, and $F_{j,V}$ is the repulsive force generated by the velocity potential field of the j-th obstacle.

$$F_{j,x} = -\nabla_x \left\{ \frac{1}{2}\eta_j \left(\frac{1}{d_j(x)} - \frac{1}{Q_j^*} \right)^2 d(x,G)^2 + \frac{1}{2}\eta_V {V_{R,obs}}^2 \right\} = F_{j,x}1 + F_{j,x}2 + F_{j,x}3 \tag{8}$$

$$F_{j,x}1 = -\eta_j \left(\frac{1}{d_j(x)} - \frac{1}{Q_j^*} \right) \frac{d_j(x)^2}{d_j(x)^2} \tag{9}$$

$$F_{j,x}2 = \eta_j \left(\frac{1}{d_j(x)} - \frac{1}{Q_j^*} \right)^2 d_j(x) e_{R,goa} \tag{10}$$

$$F_{j,x}3 = \pm \eta_V V_{R,obs} \frac{V_{R,obs\perp} e_{R,obs\perp}}{d_j(x)} \tag{11}$$

Where, "$\pm$" stands for left and right directions; "+" stands for right direction and "—" stands for left direction.

By substituting Equations (13), (14) and (15) into Equation (12), it could be referred,

$$F_{j,x} = -\eta_j \left(\frac{1}{d_j(x)} - \frac{1}{Q_j^*} \right) \frac{d_j(x)^2}{d_j(x)^2} + \eta_j \left(\frac{1}{d_j(x)} - \frac{1}{Q_j^*} \right)^2 d_j(x) e_{R,goa} \pm \eta_V V_{R,obs} \frac{V_{R,obs\perp} e_{R,obs\perp}}{d_j(x)} \tag{12}$$

Similarly, it could be acquired,

$$F_{j,V} = -\nabla_V \left\{ \frac{1}{2}\eta_j \left(\frac{1}{d_j(x)} - \frac{1}{Q_j^*} \right)^2 d(x,G)^2 + \frac{1}{2}\eta_V {V_{R,obs}}^2 \right\} = -\eta_V V_{R,obs} e_{R,obs} \tag{13}$$

Furthermore, the repulsive force of the obstacle to the ship could be obtained,

$$F_{rep,j}(x,V) = -\eta_j \left(\frac{1}{d_j(x)} - \frac{1}{Q_j^*} \right) \frac{d_j(x)^2}{d_j(x)^2} + \eta_j \left(\frac{1}{d_j(x)} - \frac{1}{Q_j^*} \right)^2 d_j(x) e_{R,goa} + \eta_V V_{R,obs} \frac{V_{R,obs\perp} e_{R,obs\perp}}{d_j(x)} - \eta_V V_{R,obs} e_{R,obs} \tag{14}$$

ISSN 2616-5805 Vol. 5, Issue 3: 23-30, DOI: 10.25236/AJMS.2024.050304

It can be seen from the formula that $F_{j,x}3 = \pm\eta_V V_{R,obs} \frac{V_{R,obs\perp} e_{R,obs\perp}}{d_j(x)}$ is the force perpendicular to the line connecting the position of the own ship and the target ship, which is mainly used to control the left or right turn of the own ship relative to the target ship, as shown in Figure 2.

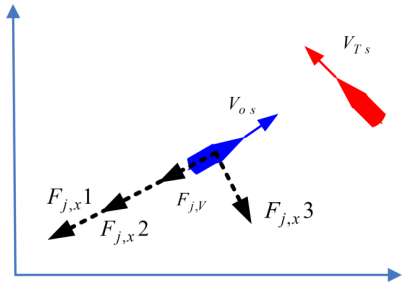

Figure 2: Schematic diagram of improved APF

2.3. Calculation of Q_j^* value of repulsion potential field

The value of the Q_j^* parameter of the repulsion potential field is divided into the calculation of the range of static obstacles such as shallows and the range of dynamic obstacles such as ships. The calculation of the range of action of static obstacles such as shallows mainly considers the range of free ships based on own ship's maneuverability.

Similarly, the calculation of the range of action of dynamic obstacles such as ships mainly considers the coordination range of the free ship range of the own ship and the free ship range of the target ship based on the maneuverability of the ship. To analyze and compare the application of the ship domain model, in the open water, this paper chooses Wang Ning and others to establish a self-organizing ship domain recognition model based on the fuzzy neural network method, combining the ship's maneuverability and the situation of the ship's encounter [14].

3. Computer experiment

The initial parameters of the test are set as follows: the initial coordinates of the own ship (Os) are (1500, 10000), the initial speed of the ship is 10m/s, the initial course of the ship is 50°, and the coordinates of the destination are (17500, 21000). The parameters of the three interfering ships (Ts1, Ts2 and Ts3) are set as follows: the initial coordinates are (4000, 9000), (13000, 11000) and (18500, 7000) respectively, and the speed is 4.0m/s, 7.0m/s and 9m /s, the heading is 45°, 320° and 358°. The positions of the 4 static obstacles (Obs1, Obs2, Obs3 and Obs4) are (12500, 18500), (18500, 15000), (7000, 11000) and (4000, 17000) respectively.

The trajectory of the collision avoidance path between ships in the presence of multiple obstacles is shown in Figure 3. During the collision avoidance process, the motion trajectories of the Os and Ts1, Ts2, and Ts3 are displayed with orange, pink, blue and green lines respectively. The figure shows that the ship started from the initial position and was successively affected by interference Ts1, Obs4, Ts2, Ts3, and Obs1. After taking appropriate steering and collision avoidance actions, it arrived at the destination smoothly.

In the collision avoidance path planning, the course change curve of the ship and the three interfering ships in the encounter is shown in Figure 4. Obviously, it can be seen that the course of the Os and the Ts3 have changed greatly, and there are many extreme points on the curve. In combination with Figure 3, it can be seen that the two ships are subject to more external interference and greater influence, especially the navigation of Ts3 is severely affected by other obstacles including the ship, and its trajectory is seriously deviated from the initial track. For the Os, all three heading extreme points occurred during the encounter with the interfering ship.

ISSN 2616-5805 Vol. 5, Issue 3: 23-30, DOI: 10.25236/AJMS.2024.050304

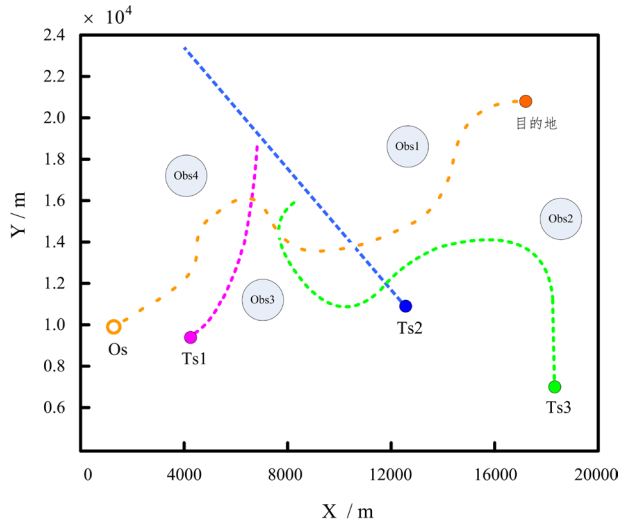

Figure 3: The trajectory of collision avoidance between ships in the presence of multiple obstacles

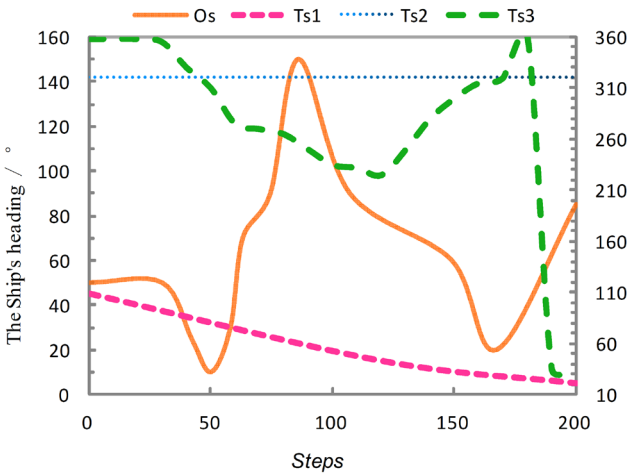

Figure 4: The course change curve of each ship during the collision avoidance process

According to Figure 3, the Os first formed a chasing situation with the Ts1. At the same time, combined with the distance between the Obs3 and the Obs4, the ship first redirected to the left. During this time, the Ts1 was affected by the repulsion of the Obs3 and moved. The trajectory deviates slightly to the left, and the heading slowly decreases; after completing the chase (step 58), affected by the repulsive force of the Obs4, quickly change direction to the right. At the 86th step, it formed a cross encounter situation with the Ts2. The Os changed its direction to the right and passed through the stern of the Ts2. Afterwards, due to the attractive force of the destination, the ship quickly turns left and its course is greatly reduced. On the way to the destination, when running to the end 167 steps, affected by the repulsive force of the Obs1, the ship's course turns right again and gradually reaches the destination.

Figure 5 is a historical graph of the distance change between own ship and the interference ships during collision avoidance. It can be seen from Figure 5 that during the entire collision avoidance process, the closest distance between the Os and the Ts1 is 2000m, the closest distance to the Ts2 is 2500m, and the closest distance to the Ts3 is 1800m.

ISSN 2616-5805 Vol. 5, Issue 3: 23-30, DOI: 10.25236/AJMS.2024.050304

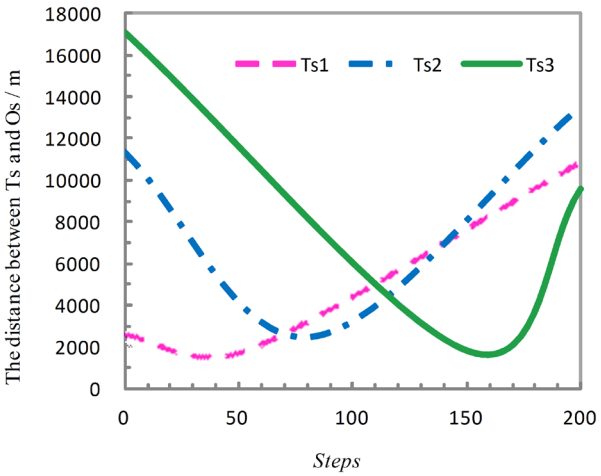

Figure 5: The curve of distance change between the target ship and own ship during collision avoidance

The experiment verifies that the improved artificial potential field algorithm fused with velocity potential field can effectively deal with the collision avoidance path planning problem of ships in complex waters with coexistence of dynamic and static targets. The path obtained by this algorithm has high smoothness, can meet the requirements of the "Regulations", and can effectively solve the problems of unreachable targets that are easy to appear in the traditional artificial potential field method.

4. Conclusion

The relative speed of the unmanned ship and the obstacle is integrated into the APF with distance as the element, the potential field method with speed is constructed, and which is applied to the narrow waterway where moving and static targets coexist. The autonomous ship collision avoidance dynamic path planning is in progress. Computer simulation verifies that the algorithm can effectively deal with the collision avoidance path planning problem of ships in complex waters with coexistence of dynamic and static targets. It is shown that the proposed algorithm is effective and feasible, and the path is smoothness. It can be satisfied the requirements of the "Regulations".

On the other hand, the algorithm can effectively solve the problem of unreachable targets that are easy to appear in the traditional artificial potential field method.

Ackowledgments

This work was supported by the Science and Technology Innovation Fund Project of Jiangsu Maritime Institute under Grant 2022kjcx-04, 2022zkZD02 and 2022zkZD03, and the Planning project of Huang Yanpei Vocational Education Thought Research under Grant ZJS2024YB295 by the Research on Teacher Team Construction of Interdisciplinary Integration in Maritime Vocational Colleges under the Background of Intelligent Ships.

References

[1] Hongguang Lyu, Yong Yin. Fast path planning for autonomous ships in restricted waters[J]. Appl. Sci. 2018, 8, 2592.
[2] Agnieszka Lazarowska. Ship's trajectory planning for collision avoidance at sea based on ant colony optimisation[J]. The Journal of Navigation, 2015, 68, 291-307.
[3] Yuanqiang Zhang, Guoyou Shi, Hu Liu, et al. Decision supporting for ship collision avoidance in restricted waters[J]. International Journal of Simulation and Process Modelling, 2020, 15(1-2): 40-51.
[4] Lou Jiankun, Wang Hongdong, Wang Jianyao. Intelligent evolution method of collision avoidance algorithm for unmanned boats in real sea based on machine learning[J]. Chinese Ship Research, 2021, 16(1): 65-73.

ISSN 2616-5805 Vol. 5, Issue 3: 23-30, DOI: 10.25236/AJMS.2024.050304

[5] Fang Deng, Leilei Jin, Xiuhui Hou, et al. COLREGs: compliant dynamic obstacle avoidance of usvs based on the dynamic navigation ship domain[J]. J. Mar. Sci. Eng., 2021, 9, 837.
[6] Zhou Wei, Guo Xuexun, Pei Xiaofei, et al. Research on intelligent vehicle path planning and tracking control based on RRT and MPC[J]. Automotive Engineering, 2020, 42(09): 1151-1158.
[7] Chen Tianyuan, Yuan Wei, Yu Menghong. Research on autonomous dynamic collision avoidance method for unmanned ships based on collective guidance and dynamic window constraints[J]. China Shipbuilding, 2020, 61(3): 176-185.
[8] Liu Jiandao, Liu Wen, Zhang Yingjun, et al. Autonomous collision avoidance algorithm for unmanned surface craft based on improved dynamic window method[J]. Journal of Shanghai Maritime University, 2021, 42(2): 1-7.
[9] Haitong Xu, Miguel A. Hinostroza, C. Guedes Soares. Modified vector field path-following control system for an underactuated autonomous surface ship model in the presence of static obstacles[J]. J. Mar. Sci. Eng., 2021, 9, 652.
[10] Song L., Su Y., Dong Z., et al. A two-level dynamic obstacle avoidance algorithm for unmanned surface vehicles[J]. Ocean. Eng., 2018, 170, 351–360.
[11] Man-Chun Lee, Chung-Yuan Nieh, Hsin-Chuan Kuo, et al. An automatic collision avoidance and route generating algorithm for ships based on field model[J]. Journal of Marine Science and Technology, 2019, 27(2): 101-113.
[12] Sun Yaodong. Research on Intelligent Planning of Ship Navigation Path [D]. Dalian Maritime University, Dalian, 2018, 3.
[13] KHATIB O. Real-time obstacle avoidance for manipula-tors and mobile robots[J]. The international journal of robotics research, 1986, 5(1): 90-98.
[14] Wang, N. A novel analytical framework for dynamic quaternion ship domains[J]. J. Navig., 2013, 66, 265-281.